SMALL ANGLE X-RAY SCATTERING STUDY OF THE POROSITY IN CHARCOALS

J. L. Casteel, O. Allan Pringle, J. S. Lin,[1] and *P. W. Schmidt*

Physics Department, University of Missouri, Columbia, Mo. 65211

Dwight H. Slocum[2] and *E. Allen McGinnes, Jr.*

School of Forestry, Fisheries, and Wildlife, University of Missouri, Columbia, Mo. 65211

and

Frank C. Beall[3]

School of Forest Resources
The Pennsylvania State University, University Park, Pa. 16802

(Received 7 February 1977)

ABSTRACT

Small angle X-ray scattering data have been obtained for a series of charcoal samples produced by heating in a laboratory furnace under conditions chosen to simulate those encountered in commercial kilns. The scattering curves suggest that the samples contain three types of pores: (1) relatively large pores, with dimensions of the order of a few microns, which are similar to the pores in the lignin-cellulosic skeleton of the wood from which the charcoal was made; (2) platelet-like pores, with one dimension that does not exceed 2 or 3 nm and with the other two average dimensions being considerably larger; and (3) small pores, which have no dimensions greater than about 1 or 2 nm. For charcoals heated to 400 C, only the large pores are present in appreciable numbers. As the maximum heating temperature is increased, the platelet and small pores make an increasing contribution to the scattering. Estimates have been made of the fraction of the volume of the porous charcoal occupied by each of the three types of pores.

Keywords: *Quercus alba, Carya ovata,* charcoal, X-ray analysis, ultrastructure, cell-wall porosity.

INTRODUCTION

Small angle X-ray scattering provides information about the submicroscopic structure of materials (Guinier et al. 1955; Schmidt 1971). Dimensions from about 1 through 500 nm can be conveniently studied. The resolution thus is higher than is possible with an optical microscope or with most scanning electron microscopes. A few years ago we described a small angle X-ray scattering study of some oak charcoals produced in Missouri-type kilns (Von Bastian et al. 1972). The information that we obtained about the submicroscopic pore structure of these charcoals would have been difficult to find by electron microscopy.

We have now completed some additional measurements of the small angle X-ray scattering from oak and hickory charcoals. Unlike the charcoals studied in our earlier work, which were obtained from regular runs of commerical charcoal kilns, the samples discussed below were produced in a laboratory furnace under conditions chosen to resemble those occurring in commercial production. Because of the closely controlled heating possible with the laboratory furnace,

[1] Present Address: Metals and Ceramics Division, Oak Ridge National Laboratory, P. O. Box X, Oak Ridge, TN 37830.

[2] Present Address: Weyerhaeuser Company, Tacoma, WA 98401.

Wood and Fiber, 10(1), 1978, pp. 6–18

the conditions under which the samples were prepared were much better known than is possible with commercial charcoals. The information obtained about the effect of the conditions of preparation on submicroscopic pore structure can therefore be expected to be more reliable than in our earlier work. In addition, we now have developed new techniques for analysis of the scattering data. With these new methods we have been able to obtain more quantitative information from the data than was possible previously.

As we explain below, the scattering data suggest that there are three different kinds of pores in the charcoals heated at temperatures of 400 C and above. First, there are relatively large pores that have dimensions of the order of microns and that are similar to the pores in the lignin skeleton of the wood from which the charcoal was produced. In addition, the scattering curves provide evidence for two other kinds of pores, which will be called platelet pores and small pores. One dimension of the platelet pores does not exceed 2 or 3 nm, while the other two dimensions are considerably larger. None of the dimensions of the small pores are greater than 1 or 2 nm.

For charcoal heated at 400 C, most scattering comes from the large pores. When the charcoals are heated at higher temperatures, a greater fraction of the total scattering is due to the platelet pores and the small pores, while there is only a relatively small increase in scattering from the large pores.

Although the existence of these three kinds of pores must be considered somewhat tentative until the presence of platelet pores and small pores is confirmed by other techniques besides small angle X-ray scattering, with this pore structure we have been able to provide a reasonable explanation of the scattering curves from the charcoal samples.

Summary of small angle X-ray scattering techniques

A schematic diagram of an apparatus for X-ray scattering studies is shown in Fig. 1. The beam from the X-ray tube T is defined by the slits S_1 and S_2 and strikes the sample S. Although most of the X-rays either pass through the sample without being affected or are absorbed in the sample by the process of photoelectric absorption, a small fraction of the beam is re-emitted in other directions besides that of the incident beam. These rays are called the scattered rays. The diagram shows a ray scattered at an angle θ, called the scattering angle, with respect to the incident beam. The intensity of the X-rays scattered at different angles θ is determined by the structure of the sample. In scattering studies, the scattered radiation is measured as a function of the scattering angle θ. Then, by analysis of the scattering data, information is obtained about the structure of the sample.

In the apparatus shown in Fig. 1, the two slits S_3 and S_4 and the counter C are mounted on an arm that rotates about an axis through the sample S and perpendicular to the plane of the drawing. By rotation of this arm, the scattered intensity can be measured at different scattering angles.

X-rays are scattered primarily by electrons, and the observed X-ray scattering intensity is the result of differences in electron density in different regions of the sample. When regions with different electron density have dimensions of the same magnitude as the X-ray wavelength, the scattering is most intense at angles of 10 degrees or more. The atomic structure in solids and liquids ordinarily is of

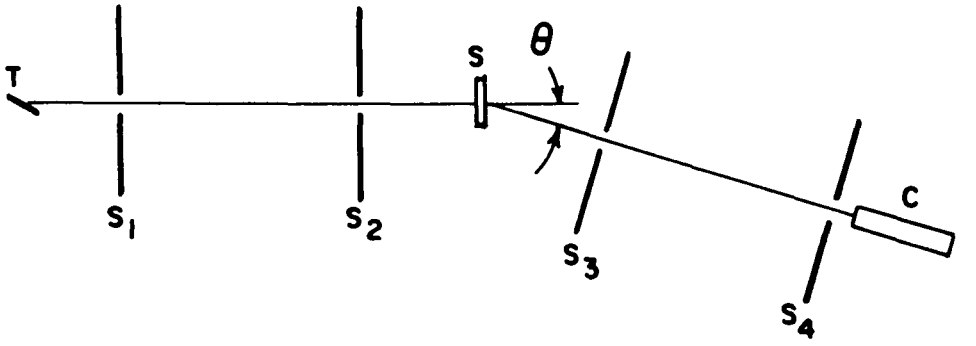

FIG. 1. A schematic diagram of a typical scattering system. X-Rays from the tube T are defined into a beam by slits S_1 and S_2 and strike the sample S. Slits S_3 and S_4 and the proportional counter C permit measurement of the scattered intensity as a function of the scattering angle θ.

the same magnitude as the wavelengths normally employed for X-ray scattering and diffraction. The angles of interest for X-ray diffraction and scattering for the usual liquids and solids thus are usually greater than 10 degrees.

On the other hand, if the inhomogeneities in the electron density are larger than the X-ray wavelength, the scattered intensity is appreciable only at scattering angles of a few degrees or less. Small angle X-ray scattering, unlike ordinary X-ray diffraction, thus provides information about inhomogeneities in electron density that are appreciably larger than the normal interatomic distances in dense materials.

At these small scattering angles, the scattering is not affected by structure with dimensions of only a few tenths of a nanometer (Guinier et al. 1955, pp. 3–4), and therefore, in the analysis of small angle X-ray scattering data, the atomic structure can be neglected, and the sample can be assumed to consist of two phases, each of which has a constant electron density. For analysis of the scattering data from the charcoal samples, one phase will be assumed to be carbon, with a constant electron density (i.e., with a constant number of electrons per unit volume), and the other phase will be considered to be pores containing air. Since scattering from the air is very weak, the electron density in the pores can be set equal to zero.

Methods for analyzing scattering curves

Some properties of the scattering from porous systems like charcoals will now be reviewed. Since the methods used for interpreting our recent scattering measurements are considerably different from the techniques employed in our earlier work (Von Bastian et al. 1972), the procedures used below will be discussed in some detail. Readers interested only in the results of our scattering studies can skip most of this section.

The scattering angle θ can be conveniently expressed by the quantity $h = 4\pi\lambda^{-1}\sin(\theta/2)$, where λ is the X-ray wavelength. In the small-angle region, $\sin(\theta/2) \simeq \theta/2$, and thus in the analysis of the small angle scattering curves, h can be considered proportional to θ. (In the equation defining h, the scattering angle θ must be expressed in radians.)

The form and size of the pores can be characterized by three average pore dimensions—a length, a width, and a height. For scattering angles at which D_{min}, the smallest of these three average dimensions, satisfies the condition

$$hD_{min} > 3.5, \tag{1}$$

(Bragg et al. 1963), the scattered intensity I(h) can be approximated by

$$I(h) = 2\pi\rho^2 I_e S h^{-4} \tag{2}$$

where ρ is the electron density in the carbon phase, I_e is the intensity scattered by a single electron, and S is the total surface area separating the pores and the carbon in the sample. (Guinier et al. 1955, p. 80 and p. 17).

When a pore has the form of a platelet, the two dimensions D_1 and D_2, which define the platelet face, will both be much larger than the platelet thickness $a = D_{min}$. Thus, for platelets there will be an interval of scattering angles for which $hD_1 \gg 1$ and $hD_2 \gg 1$, even though (1) is not satisfied. If the platelet pores have different thicknesses, it is convenient to introduce the platelet thickness distribution p(a), which is defined to have the property that p(a)da is the probability that a pore will have a thickness in the interval between a and a + da. For scattering angles for which $hD_1 \gg 1$ and $hD_2 \gg 1$ but for which (1) may or may not be fulfilled, the average scattering from a sample of N randomly oriented platelet pores can be expressed (Pringle and Schmidt 1977) in the form

$$I(h) = 2\pi N\rho^2 \langle V_{pl}\rangle \frac{\langle a^2\rangle}{\langle a\rangle} h^{-2} I_e G(h) \tag{3}$$

where

$$\langle a^n\rangle = \int_0^\infty a^n p(a)\, da, \tag{4}$$

$\langle V_{pl}\rangle = a\langle a\rangle$ is the average volume of a platelet, a is the average surface area of *one* face of the platelet, and

$$G(h) = \frac{1}{\langle a^2\rangle}\int_0^\infty a^2 p(a) \frac{\sin^2(ha/2)}{(ha/2)^2}\, da. \tag{5}$$

(In these equations, the average over platelet areas is assumed to be independent of the average over thicknesses.) The thickness distribution p(a) is assumed to satisfy the condition

$$\int_0^\infty p(a)\, da = 1.$$

When $h\langle a\rangle \ll 1$, $G(h) \approx 1$, while if $h\langle a\rangle \gg 1$, (3) can be shown to reduce to (2).

Thus, when $h\langle a\rangle$ is small, the scattered intensity from a platelet pore will be proportional to h^{-2}, while for h values large enough that $h\langle a\rangle \gg 1$, the scattering is proportional to h^{-4}, as specified by (2).

When D_{max}, the largest of the three dimensions characterizing a pore, is so small that for the observed scattering angles hD_{max} is not large, the scattering $I_s(h)$ from a single pore can be approximated by the expression (Guinier et al. 1955, p. 7, p. 16, p. 25):

$$I_s(h) = (V_s)^2 \rho^2 I_e e^{-h^2R^2/3} \tag{6}$$

where V_s is the volume of the pore, and R, the radius of gyration of the pore, is a length that characterizes the size of the pore. Since $R < D_{max}$ (Guinier et al.

1955, pp. 24–28), when $hD_{max} \ll 1$, the scattering from the small pores is nearly independent of h. For $hD_{max} > 1$, (6) may no longer be a good approximation. When $hD_{max} > 3.5$, $I_s(h)$ approaches the h^{-4} dependence given by (2).

As has been mentioned previously, these properties of the scattered intensity assume that the pores are so large that the scattered intensity occurs at scattering angles for which the carbon in the charcoal can be considered to have a constant electron density. At scattering angles greater than about 10 degrees, the scattered intensity begins to be affected by the atomic structure of the sample, and the assumption of constant electron density is no longer valid.

The platelet pores and the small pores will be assumed to scatter independently. Then the total scattered intensity from N pores of a given type will be N times the scattering from a single pore.

For the analysis of the charcoal scattering curves, the scattered intensity will be assumed to be the superposition of the scattering from large pores, platelet pores, and the small pores, and the thickness of the platelet pores will be assumed to be small enough that the observed intensity from these pores is proportional to h^{-2}. The scattered intensity from the charcoal sample then can be expressed

$$I(h) = \alpha h^{-4} + \beta h^{-2} + \gamma e^{-(1/3)h^2\langle R^2\rangle} \tag{7}$$

where α, β, and γ represent the contributions from the large pores, the platelet pores, and the small pores, respectively. In the development of (7), the assumption was made that

$$e^{-(1/3)h^2\langle R^2\rangle} = \langle e^{-(1/3)(hR)^2}\rangle .$$

This assumption is satisfied when hR is small enough that (6) is a good approximation for the scattering from the small pores.

In (7), and in the rest of this section, brackets denote averages over the charcoal sample.

If there are n_l large pores per unit volume, and if $\langle S_l\rangle$ and $\langle V_l\rangle$, respectively, are the average surface area and volume for a large pore, $S = n_l\langle S_l\rangle V$, and $c_l = n_l\langle V_l\rangle$, where V is the total sample volume, and c_l is the fraction of the volume occupied by the large pores. With these results, from (2)

$$\alpha = 2\pi\rho^2 I_e V c_l(\langle S_l\rangle/\langle V_l\rangle). \tag{8}$$

Let N_{pl} be the number of platelet pores per unit volume. Then $c_{pl} = n_{pl}\langle V_{pl}\rangle$, where c_{pl} is the fraction of the sample volume occupied by the platelet pores. Similarly, if c_s is the fraction of the sample volume occupied by the small pores, $c_s = n_s\langle V_s\rangle$, where n_s is the number of small pores per unit volume. Then if the platelet pores and the small pores scatter independently, and if $h\langle a\rangle \ll 1$, from (3) and (6),

$$\beta = 2\pi\rho^2 I_e V c_{pl}\frac{\langle a^2\rangle}{\langle a\rangle} \tag{9}$$

and

$$\gamma = I_e\rho^2 V c_s\frac{\langle V_s^2\rangle}{\langle V_s\rangle} . \tag{10}$$

TABLE 1. *Heating conditions for the charcoal samples.*

Sample	Maximum temperature °C	Heating rate °C/Hr	Time to reach maximum temperature Hr	Time at maximum temperature Hr	Total heating time Hr
250S Oak	250	1.5	167	0	167
250S Hickory	250	1.5	167	0	167
400S Oak	400	5	80	0	80
400S Hickory	400	5	80	0	80
600S Oak	600	30	20	0	20
600S Hickory	600	30	20	0	20
600L Oak	600	30	20	100	120
600L Hickory	600	30	20	100	120
800S Oak	800	130	6	0	6
800S Hickory	800	130	6	0	6
800L Oak	800	130	6	114	120
800L Hickory	800	130	6	114	120

METHODS

Sample preparation and scattering measurements

The charcoals were prepared from heartwood samples of white oak (*Quercus alba* L.) and hickory [*Carya ovata* (Mill.) K. Koch] in a laboratory furnace at The Pennsylvania State University. The heating conditions were selected to approximate those likely to be encountered in commercial charcoal kilns.

The samples were inserted in the furnace when it was at room temperature. The furnace temperature was then raised at a uniform rate. Some samples were removed from the furnace as soon as the temperature reached a desired value, while others were held in the furnace at the maximum temperature for about 100 hours. The code letters S and L, respectively (for "short" and "long" heating times), specify the two types of heat treatment. The numbers used in the designations of the samples indicate the maximum temperature of heating (in degrees C). For example, the 600L sample was raised to 600 C and held at this temperature, while the 600S sample was removed from the furnace as soon as the temperature reached 600 C. Heating conditions are shown in Table 1.

Since our earlier study of charcoal suggested that, at least to a first approximation, the small angle scattering was isotropic—i.e., independent of whether the sample was a radial, longitudinal, or tangential section, all of the charcoal samples were ground in a mortar and pestle. The powders were ground fine enough to pass through a 40-mesh screen.

Results of our small angle X-ray scattering study of unheated samples of the woods used to make the charcoals are reported in another paper (Casteel et al. 1977).

X-ray scattering measurements

The scattering curves were obtained with a copper-target X-ray tube, a proportional counter, and a Kratky collimation system (Kratky and Skala 1958) with a slit arrangement equivalent to that used in our earlier investigation of charcoal. (Although the slits in the Kratky camera are arranged differently from those in Fig. 1, the results obtained from the two systems are equivalent.) A linear am-

plifier and pulse height analyzer were used with the proportional counter to select only the counts produced by the copper K-α X-rays, which have a wavelength 0.154 nm.

After the background scattering had been subtracted, the scattering curves were corrected for the effects of the length and width of the collimating slits, and the uncertainties in the corrected data were calculated (Lin et al. 1974; Taylor and Schmidt 1967). The incident intensity was monitored in the same way as in our earlier studies of charcoal.

The equations discussed in the previous section neglect the weakening of the X-ray beam which results from photoelectric absorption in the sample. This attenuation can conveniently be described (Compton and Allison 1935) by the transmission τ,

$$\tau = I/I_0 = e^{-(\mu_m M/A_0)} \tag{11}$$

where I is the intensity of the undeviated X-ray beam after it has passed through the sample; I_0 is the intensity of the X-ray beam incident on the sample; μ_m is the mass absorption coefficient of the material of which the sample is composed; A_0 is the area of the sample illuminated by the incident beam; and M is the mass of the illuminated portion of the sample.

To find the transmission τ, the collimation system was set at zero scattering angle and the intensity was measured with the sample in the beam and also when it was removed.

Because of photoelectric absorption, the intensity of all measured scattering curves is reduced by the factor τ. To correct for this absorption in the samples, we divided each scattering curve by the transmission measured for the sample. The resulting corrected curves give the scattering that would have been obtained for the nonabsorbing sample that was assumed in the development of Equations (1)–(10).

Since, as shown by (8)–(10), the scattered intensity is proportional to the sample volume, allowance must be made for differences in sample volume when the scattering curves from different samples are compared. Although all scattering curves were obtained with the same setting of the collimating slits, so that the illuminated area A_0 of the sample was the same for all scattering curves, the sample volumes differed because the thickness of the sample in a direction parallel to the incident beam varied from sample to sample. To allow for this effect, we expressed the sample volume in terms of the mass per unit area by use of the relation

$$V = \frac{M}{A_0}\frac{A_0}{d}$$

where d is the density of the powdered sample. With (11) and the tabulated value of the mass absorption coefficient μ_m for carbon, M/A_0 can be calculated from measured values of the transmission τ. Measurements showed that for the oak and hickory charcoals, d is approximately 0.60 and 0.75 gm/cm^3, respectively. To allow for the differences in sample volume, we therefore divided all intensities by the values of $\log_{10}(1/\tau)$. Then if all samples of a given wood can be assumed to have the same density d, as our measurements suggest is at least approximately

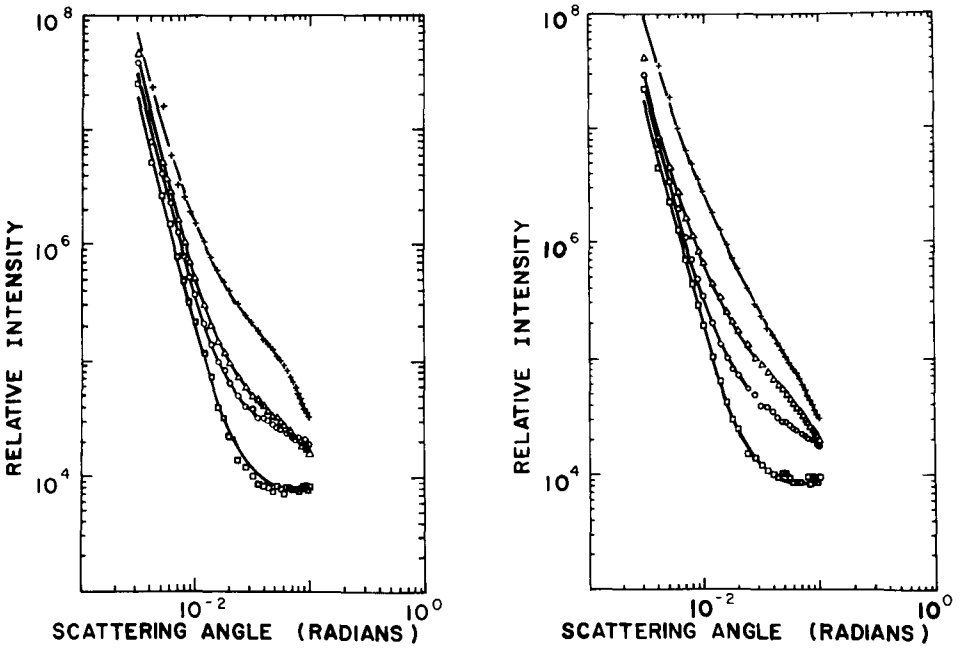

FIG. 2. Corrected scattering curves for the 400S (squares), 600S (circles), 800S (triangles) and 800L (crosses) oak charcoals. The curves are least-squares fits of Eq. (7) to the data points.

FIG. 3. Corrected scattering curves for the 400S (squares), 600S (circles), 800S (triangles), and 800L (crosses) hickory charcoals. The curves are least-squares fits of Eq. (7) to the data points.

the case, the corrected scattering curves will correspond to samples with equal volume. (The area A_0 is the same for all samples.)

Measurements of the scattering from the same charcoal for samples with different thicknesses suggested that the effects of multiple scattering were not appreciable.

RESULTS

Analysis of the scattering curves

Scattering curves for the 400S, 600S, 800S, and 800L samples are shown in Figs. 2 and 3 for the oak and hickory charcoals, respectively. The curves have been corrected for background scattering, length and width collimation effects, absorption, and variation in sample thickness. The symbols show intensities obtained from the scattering measurements, and the lines are curves obtained by making a least-squares fit of (7) to the corrected experimental scattering curves.

The scattering curves for the 250S oak and hickory samples are not shown, since they were essentially the same as the curves for the corresponding oak and hickory powdered wood samples which have been discussed elsewhere (Casteel et al. 1977).

The scattering curves for the 600L oak and hickory samples have been discussed previously (Pringle and Schmidt 1977). For these curves, a distribution of platelet thicknesses could be calculated. The fact that this distribution can be obtained implies that the thickness of the platelet pores is not negligible.

TABLE 2. *Values of α, β, γ, R, and S/M.*

Sample	α	β	γ	R nm	S/M m^2/gm
400S Oak	0.44×10^{-4}	0.54	0.066×10^{-5}	0.0001	0.37
400S Hickory	0.39	0.63	0.080	0.0002	0.33
600S Oak	0.64	1.57	0.24	0.25	0.54
600S Hickory	0.52	2.1	0.26	0.30	0.44
600L Oak	0.58	—	—	—	0.49
600L Hickory	0.49	—	—	—	0.41
800S Oak	0.79	3.0	0.31	0.39	0.66
800S Hickory	0.57	6.7	0.53	0.48	0.48
800L Oak	1.31	13.83	1.33	0.59	1.10
800L Hickory	1.55	34.	0.31	0.45	1.30

When h is expressed in nm with $\gamma = 0.154$ nm, and the above values of α, β, and γ are used in Eq. (7), the intensities given by the curves in Figs. 2 and 3 are obtained. The angle θ in h must be expressed in radians.

Although the intensities of the curves in Figs. 2 and 3 are given in arbitrary units, the same units are used for all the curves, so that intensities scattered by different samples can be compared. Intensity ratios are accurate within about ±5%.

Values of α, β, γ, and R obtained from the least-squares fits are listed in Table 2.

Values of α are also shown in Table 2 for the 600L oak and hickory samples. As has been mentioned previously, the thickness of the platelet pores in these samples cannot be considered negligible, and so β and σ, which are meaningful only when the thickness of the platelet pores is not appreciable, cannot be calculated. However, the constant α, which specifies the specific surface of the large pores, still can be evaluated.

The specific surface S/M for the samples can be obtained from the values of α. From (2) and (8)

$$\alpha = 2\pi\rho^2 I_e A_0 (M/A_0)(S/M). \tag{12}$$

The quantity $I_e A_0$ was evaluated from the measured scattering curve for a concentrated silica suspension (Patel and Schmidt 1971), and M/A_0 was calculated from the measured transmission by use of (11). The calculated specific surface values in m^2/gm are given in Table 2. The uncertainty in these results is estimated to be ±10%.

Estimates of the fraction of the volume occupied by different types of pores

To test the consistency of our analysis of the scattering curves, we estimated the fraction of the volumes occupied by the large and small pores and by the platelet pores. The fact that these volume fractions are not unreasonable shows that the model we suggest for the charcoal pore structure is not inconsistent with the scattering data for these samples.

First, we develop expressions for the fraction of the pore volume for each type of pore. From (8),

$$\alpha = 2\pi\rho^2 I_e V \frac{S}{M} d, \tag{13}$$

where $d = M/V$ is the density of the porous charcoal.

If, as mentioned in Section 2, the charcoal is considered to be a two-phase system consisting of pores in a carbon skeleton with density d_0,

$$d = d_0(1 - c_l - c_{pl} - c_s). \tag{14}$$

By use of (13), (9), and (10), the fractions c_{pl} and c_s of the charcoal volume that are occupied respectively by the platelet and small pores can be shown to be given by

$$c_{pl} = \frac{\beta}{\alpha} \frac{S}{M} d \left[\frac{\langle a^2 \rangle}{\langle a \rangle}\right]^{-1} \tag{15}$$

and

$$c_s = 2\pi d \frac{\gamma}{\alpha} \frac{S}{M} \left[\frac{\langle V_s^2 \rangle}{\langle V_s \rangle}\right]^{-1}. \tag{16}$$

Measurements of the densities of the porous charcoals showed that within a few percent, d was equal to 0.60 gm/cm^3 for all oak charcoals and 0.75 gm/cm^3 for all hickory charcoals in Table 2.

We used these densities and the information in Table 2 for estimating c_{pl} and c_s. For these calculations, we assumed that d_0 was 2 gm/cm^3 and that all the small pores were spheres with radii equal to the radius $\sqrt{5/3}$ R, corresponding to a uniform sphere with radius of gyration R. (Guinier et al. 1955, p. 26). Then

$$\frac{\langle V_s^2 \rangle}{\langle V_s \rangle} \simeq \frac{4\pi}{3} (5/3)^{3/2} R^3.$$

Since $\langle a^2 \rangle / \langle a \rangle$ is about 2.8 nm for the 600L charcoals (Pringle and Schmidt 1977), we used this value for $\langle a^2 \rangle / \langle a \rangle$ in the 800L oak and hickory charcoals. For all other samples we set $\langle a^2 \rangle / \langle a \rangle$ equal to 1 nm.

While these estimates of $\langle V_s^2 \rangle$ $\langle V_s \rangle$ and $\langle a^2 \rangle / \langle a \rangle$ are quite crude, we feel that they are adequate for our rough calculations of c_{pl} and c_s. In particular, they are sufficient to show that c_{pl} is always very small.

Since, as we mentioned previously, we believe that the outer part of the scattering curves of the 400S charcoals may be governed by density fluctuations in the carbon and not by small pores, we did not calculate c_s for these charcoals.

We found that c_s was 0.05 ± 0.02 for the 600S charcoals, while for the 800S and 800L samples, it varied between 0.03 and 0.01. The volume fraction c_{pl} for the platelet pores did not appreciably exceed 0.01 in any of the samples. After c_s and c_{pl} have been calculated, c_l can be obtained from (14).

DISCUSSION

The scattering data have been interpreted by considering that charcoals contain three types of pores: (1) large pores, which have dimensions of the order of microns and which are similar to the pores in the lignin skeleton of the wood from which the charcoal was made; (2) platelet-shaped pores, with thicknesses no greater than 2 or 3 nm; and (3) small pores, with no dimensions larger than about 1 or 2 nm.

While this pore structure provides a reasonable explanation for the observed

scattering, we emphasize that evidence for the existence of the platelet pores and the small pores has been obtained only from the scattering measurements. Until independent techniques can demonstrate that the charcoals contain these two types of pores, their presence must be considered tentative.

Nevertheless, this pore structure provides a reasonable explanation for the observed scattering. Our suggestion that there are platelet pores in charcoal is supported by the fact that thin planar pores have been reported in highly graphitized carbons (Pons and Tchoubar 1973).

The term "platelet" should not be understood to mean only a pore with walls that are parallel planes. The same type of scattering would be expected from any pore in which two of the average dimensions were much greater than the third. For example, the pores could be wedges instead of having parallel walls.

The values of the small-pore radius of gyration R shown in Table 2 for the 400S oak and hickory samples are too small to be meaningful. Results from the two 400S samples thus should be interpreted to mean that there are almost no small pores in these samples. The nearly constant scattering observed in the outer parts of the scattering curves for these samples thus must be attributed to some other source, such as density fluctuations within the carbon (Ruland 1971). This constant scattering is also expected to be present in the other charcoals, but it is so weak that it is masked by scattering from the small pores.

Since the values of β are so small for the 400S oak and hickory samples, in these charcoals only the large pores make an appreciable contribution to the scattering. (As was mentioned above, the nearly constant scattering in the outer part of the scattering curve is not due to small pores but to some other effect, such as density fluctuations in the carbon.)

Because the thickness of the platelet pores in the 600L oak and hickory samples was large enough that the observed scattering from the platelet pores was not proportional to h^{-2} for all angles at which the scattering from these pores was appreciable, a least-squares fit of (7) could not be made to the scattering curves for these samples. Only α could be found from the least squares fits, and therefore in Table 2 β and γ are not listed for the 600L oak and hickory charcoals.

While the ratio of the scattering from the platelet pores probably is at least as large in the 800L oak and hickory charcoals as in the corresponding 600L samples, in the 800L charcoals scattering from the small pores is large enough to mask most scattering from the platelet pores at scattering angles where the angular distribution of the scattering is affected by the platelet thickness. The constants β and γ thus could be evaluated for the 800L charcoals. However, because of the possible effects of platelet thickness, the uncertainty in the values of β and γ is somewhat greater for the 800L samples than for the other charcoals. We cannot explain why γ is so small for the 800L hickory charcoal.

Although our estimates of c_s, c_{pl}, and c_l are only approximate, we feel that with the measured values of the density d, the volume fractions can provide some useful information about the pore structure of the charcoals.

First, since d, within the experimental uncertainty of a few percent, is the same for all samples of a given wood in Table 2, in all these charcoals the same fraction of the total volume is occupied by pores. The different conditions of preparation thus affect only the relative proportions of the different types of pores. In all cases, however, only a small fraction of the volume is occupied by platelet pores.

While the density d is essentially independent of the time and temperature of heating, the specific surface S/M increases with higher temperature and longer heating time. The average dimensions of the large pores must therefore decrease as the temperature and time of heating increase, since for a fixed volume of large pores, when the specific surface becomes larger, the average dimensions of the *individual* pores must decrease.

Since c_s becomes somewhat smaller as the heating time and heating temperature increase, the effect of these increases appears to be to cause the small pores to grow in size, possibly by coalescence, with no appreciable production of new small pores. Even though we have no direct evidence, we suggest that the decrease in c_s and associated rise in S/M may be caused at least in part by the growth of some of the small pores, which may become so large that they scatter like large pores, thus leading to a decrease in c_s and an increase in S/M. (Since in the analysis of the scattering curves the intensity from the small pores is not considered to be proportional to h^{-4}, the surface area of the small pores is *not* included in S/M, which is obtained only from the intensity scattered by pores large enough that their scattering is proportional to h^{-4}.)

The specific surfaces shown in the right-hand column of Table 2 are of the order of 0.3 to 2.0 m^2/gm and thus may seem quite small for a porous material like charcoal. We wish to point out that when the values of S in Table 1 of our first study of charcoal (Von Bastian et al. 1972) are converted to m^2/gm, the specific surface values from the earlier study are of the same magnitude as those reported in Table 2 of our recent investigation. These relatively low specific surface values therefore appear to be characteristic of the charcoals which we have investigated.

While specific surface determinations by BET adsorption would certainly be of interest for these charcoals, the surface calculated from the adsorption data may not be directly comparable to the values from the scattering curves, since specific surface results shown in Table 2 refer only to the surface associated with the large pores.

Although evidence for the small and platelet pores might be obtained from electron micrographs, these pores are so small that they might not be easily observable by transmission electron microscopy.

Our scattering data suggest that while the large pores in the charcoals are related to the pore structure of the wood from which the charcoals are produced, the platelet pores and small pores are observed primarily in charcoals that have been heated appreciably. This result suggests that very possibly the origin and properties of the small and platelet pores are connected with the behavior of carbon under heat treatment, rather than with the structure of the wood from which the charcoal was made.

ACKNOWLEDGEMENTS

This research was supported by the National Science Foundation and by McIntire-Stennis Project 174, University of Missouri Agriculture Experiment Station. We are very grateful for support from the University of Missouri College of Arts and Science Computing Fund for the many calculations necessary for the correction and analysis of the scattering curves.

REFERENCES

BRAGG, R. H., M. L. HAMMOND, J. C. ROBINSON, AND P. L. ANDERSON. 1963. Small-angle scattering by pyrolytic graphite. Nature (London) 200:555–7.

CASTEEL, J. L., O. A. PRINGLE, J. S. LIN, P. W. SCHMIDT, D. H. SLOCUM, P. E. TABIRIH, AND E. A. MCGINNES, JR. 1977. Small angle X-ray scattering investigation of the submicroscopic porosity of natural and irradiated wood of white oak and hickory. Unpublished report. 10 pp.

COMPTON, A. H., AND S. K. ALLISON. 1935. X-rays in theory and experiment, 2nd ed., pp. 9–10. Van Nostrand, New York.

GUINIER, A., G. FOURNET, C. B. WALKER, AND K. L. YUDOWITCH. 1955. Small angle scattering of X-rays. J. Wiley and Sons, New York.

KRATKY, O., AND Z. SKALA. 1958. Neues Verfahren zur Herstellung von blendenstreuungsfreien Röntgen-Kleinwinkelaufnahmen. V. Ber. Bunsenges. phys. Chemie 62:73–77.

LIN, J. S., C. R. VON BASTIAN, AND P. W. SCHMIDT. 1974. A modified method for slit-length collimation correction in small angle X-ray scattering. J. Applied Cryst. 7:439–442.

PATEL, I. S, AND P. W. SCHMIDT. 1971. Small-angle X-ray scattering determination of the electron density of the particles in a colloidal silica suspension. J. Appl. Cryst. 7:50–55.

PONS, C. H., AND D. TCHOUBAR. 1973. Diffusion des rayons X aux petits angles produite par les defauts dans les carbones. Influence d'un système optique à fente limitèe en hauteur. C. R. Acad. Sci. Paris 277:679–681.

PRINGLE, O. A. JR., AND P. W. SCHMIDT. 1977. Determination of the thickness distribution for randomly oriented, independently scattering polydisperse systems of platelets. J. Colloid Interface Sci. 60:252–7.

RULAND, W. 1971. Small-angle scattering of two-phase systems: determination and significance of systematic deviations from Porod's law. J. Appl. Cryst. 4:70–73.

SCHMIDT, P. W. 1971. Small angle X-ray scattering from suspensions of particles. Soil Sci. 112:53–61.

TAYLOR, T. R., AND P. W. SCHMIDT. 1967. A method for correcting small angle X-ray scattering curves for the effects of the width of the collimating slits. Acta Physica Austriaca 25:293–296.

VON BASTIAN, C. R., P. W. SCHMIDT, P. S. SZOPA, AND E. A. MCGINNES, JR. 1972. Small angle X-ray scattering study of oak charcoals. Wood and Fiber 4:185–192.